

LETTER • OPEN ACCESS

## Intra-urban variations in land surface phenology in a semi-arid environment

To cite this article: Ben Crawford *et al* 2025 *Environ. Res. Lett.* **20** 014036

View the [article online](#) for updates and enhancements.

You may also like

- [Interactive effects between extreme temperatures and PM<sub>2.5</sub> on cause-specific mortality in thirteen U.S. states](#)  
Edgar Castro, James Healy, Abbie Liu et al.
- [Burst flooding in Singapore: an emerging urban flooding type revealed by high-temporal-resolution observations](#)  
Dave Lommen, Wang Jingyu, Hui Su et al.
- [Assessing fire danger classes and extreme thresholds of the Canadian Fire Weather Index across global environmental zones: a review](#)  
Lucie Kudláková, Lenka Bartošová, Rostislav Linda et al.

The advertisement features a blue background with circular ECS logos at the top and bottom. In the center, there's a photo of a smiling woman in a brown blazer. To her left, text details the meeting information: "UNITED THROUGH SCIENCE & TECHNOLOGY", "ECS The Electrochemical Society Advancing solid state & electrochemical science & technology", "248th ECS Meeting Chicago, IL", "October 12-16, 2025 Hilton Chicago". To the right, large text reads "Science + Technology + YOU!". At the bottom right, a call to action says "Register by September 22 to save \$\$" and "REGISTER NOW".

# ENVIRONMENTAL RESEARCH LETTERS



## OPEN ACCESS

RECEIVED  
30 September 2022

REVISED  
14 November 2024

ACCEPTED FOR PUBLICATION  
26 November 2024

PUBLISHED  
17 December 2024

Original content from  
this work may be used  
under the terms of the  
[Creative Commons  
Attribution 4.0 licence](#).

Any further distribution  
of this work must  
maintain attribution to  
the author(s) and the title  
of the work, journal  
citation and DOI.



## LETTER

# Intra-urban variations in land surface phenology in a semi-arid environment

Ben Crawford<sup>1,\*</sup> , Kathy Kelsey<sup>1</sup> , Peter Ibsen<sup>2</sup> , Amanda Rees<sup>1</sup> and Amanda Charobee<sup>1</sup>

<sup>1</sup> Department of Geography and Environmental Sciences, University of Colorado Denver, Denver, CO, United States of America

<sup>2</sup> U.S. Geological Survey, Geosciences and Environmental Change Science Center, Lakewood, CO, United States of America

\* Author to whom any correspondence should be addressed.

E-mail: [benjamin.crawford@ucdenver.edu](mailto:benjamin.crawford@ucdenver.edu)

**Keywords:** vegetation, phenology, semi-arid, urban

Supplementary material for this article is available [online](#)

## Abstract

Urban vegetation is growing in importance as cities use ‘green infrastructure’ to mitigate the impacts of climate change, reduce extreme heat, and improve human health and comfort. However, due to the heterogeneity of city landscapes, urban vegetation experiences a diverse range of environmental conditions, potentially leading to differences in growing season timing and length within cities. Here, we investigate physical drivers of urban land surface phenology and timing within a semi-arid city (Denver, CO, USA) using four years (2018–2021) of remotely sensed vegetation indices, modelled air temperature, and land cover datasets. Within the metropolitan region study area, satellite-based vegetation index measurements indicate that growing season length is variable on sub-neighborhood spatial scales. This variability is largely due to differences in the timing of fall senescence, as opposed to early season growth. Areas with substantial fractions of irrigated land cover tend to remain greener for longer, while unirrigated and cooler areas are correlated with an earlier end to the growing season (up to ~two months shorter). These findings complement those from non-arid cities where surface and air temperature are the dominant environmental control on phenological timing. Results here indicate the importance of soil moisture for phenology in semi-arid regions and suggest unique semi-arid urban growing season dynamics and temperature-vegetation feedbacks. These interactions have implications for water, heat, and vegetation management strategies to maximize ecosystem services in water-limited environments.

## 1. Introduction

Vegetation is increasingly used in cities as living infrastructure to provide ecosystem services and improve thermal comfort for residents (Lai *et al* 2019). Although vegetation can modify urban environmental conditions, local urban settings also affect vegetation growth and productivity, resulting in altered growth and seasonality (Jochner and Menzel 2015, Pretzsch *et al* 2017). As such, vegetation and urban environmental conditions interact with one another (Melaas *et al* 2016), with vegetation timing and growth controlled by local conditions, and local surroundings mediated by the presence of vegetation. To inform urban climate change mitigation

and adaptation strategies, it is critical to advance our understanding of urban climate–vegetation interactions, particularly in water-limited cities where vegetation forms critical infrastructure and demand for water can conflict with water conservation measures.

One of the most prominent effects of urbanization on vegetation is the change to phenology, the recurring seasonal cycle of biological events such as leaf-out, flowering, and leaf coloring. Vegetation phenology, which is tracked via *in situ* observations of seasonal biological events, and land surface phenology which relies on remote sensing to detect seasonal changes in vegetated areas, both indicate changes in growing season length within cities globally, particularly driven by an advance in the start of spring

(Jochner and Menzel 2015 and references therein). This advance in spring timing has resulted in longer growing seasons of a week or more in temperate cities (White *et al* 2002, Zhang *et al* 2004, Han and Xu 2013, Jochner and Menzel 2015). Collectively, such phenological changes have the potential to alter carbon uptake of vegetation (Penuelas *et al* 2009), create mismatches or temporal isolation of species among trophic levels or among plants and pollinators, with consequences for ecological and biogeochemical processes (Beard *et al* 2019), and increase the length and severity of allergy seasons (Anderegg *et al* 2021).

Globally, plant phenology is primarily driven by temperature (Myneni *et al* 1997, Chmielewski and Rötzer 2001, Parmesan and Yohe 2003) and earlier urban growing season onset has been attributed to warmer air temperatures in cities. Air temperature generally explains more than two thirds of the variability in phenology at the start of the growing season (Menzel and Fabian 1999), however, comparisons of phenological change among cities indicate that other factors, such as land cover and intensity of urbanization, interact with temperature to control urban phenology (Li *et al* 2017, Wohlfahrt *et al* 2019, Meng *et al* 2020). Investigations of intra-urban phenology variability remain rare, however early findings from *in situ* vegetation phenology studies and remotely sensed land surface phenology investigations highlight the importance of local land cover type on intra-urban variability (Mimet *et al* 2009, Melaas *et al* 2016, Zipper *et al* 2016, Parece and Campbell 2018).

Furthermore, results from water-limited natural ecosystems underscore the important role of water availability for plant phenology (Lesica and Kittelson 2010). In water-limited cities, there is limited understanding of how water availability impacts phenology in landscapes with a heterogeneous mix of vegetation types (i.e. trees, irrigated turf, unirrigated grasses).

Although recent studies suggest temperature interacts with a multitude of environmental factors to influence urban vegetation growth, to our knowledge there have been no prior studies that focus on physical drivers of intra-urban phenology within semi-arid cities, which are now home to one in three urban residents globally (Cherlet *et al* 2018). Additionally, knowledge of intra-urban variations is essential to address unequal exposure to urban climate hazards and leverage urban vegetation as a model for future vegetation dynamics outside of urban settings.

To address this knowledge gap, we investigate spatial variability of land surface phenology within the semi-arid Denver, USA metropolitan urban landscape to characterize the role of air temperature, land cover, and irrigation as physical drivers of the start and end of the growing season.

## 2. Methods & materials

### 2.1. Study region

The study region encompasses 2117 km<sup>2</sup> of the greater Denver metropolitan area (metro area hereafter; figure 1), located in a high elevation shortgrass prairie ecosystem (mean elevation 1600 m asl) at the edge of the Rocky Mountains. The region's climate is classified as semi-arid, continental (Köppen classification BSk), characterized by hot summers and cold winters. The metro area is home to approximately 3.2 million people with a mean population density of 277 people per km<sup>2</sup>. The Denver metro area is an ideal study site to investigate land surface phenology in semi-arid urban areas due to the wide variety of managed green spaces, including parks and residential landscapes, and unmanaged land, all of which interact with its background semi-arid setting in unique ways. Denver also experiences four distinct seasons, with notable temperature and precipitation fluctuations, which are essential for capturing seasonal phenological changes. Collectively, this creates a range of microclimates and habitats in the metro area, offering a unique opportunity to study interactions between urbanization and land surface dynamics across a multitude of environmental gradients.

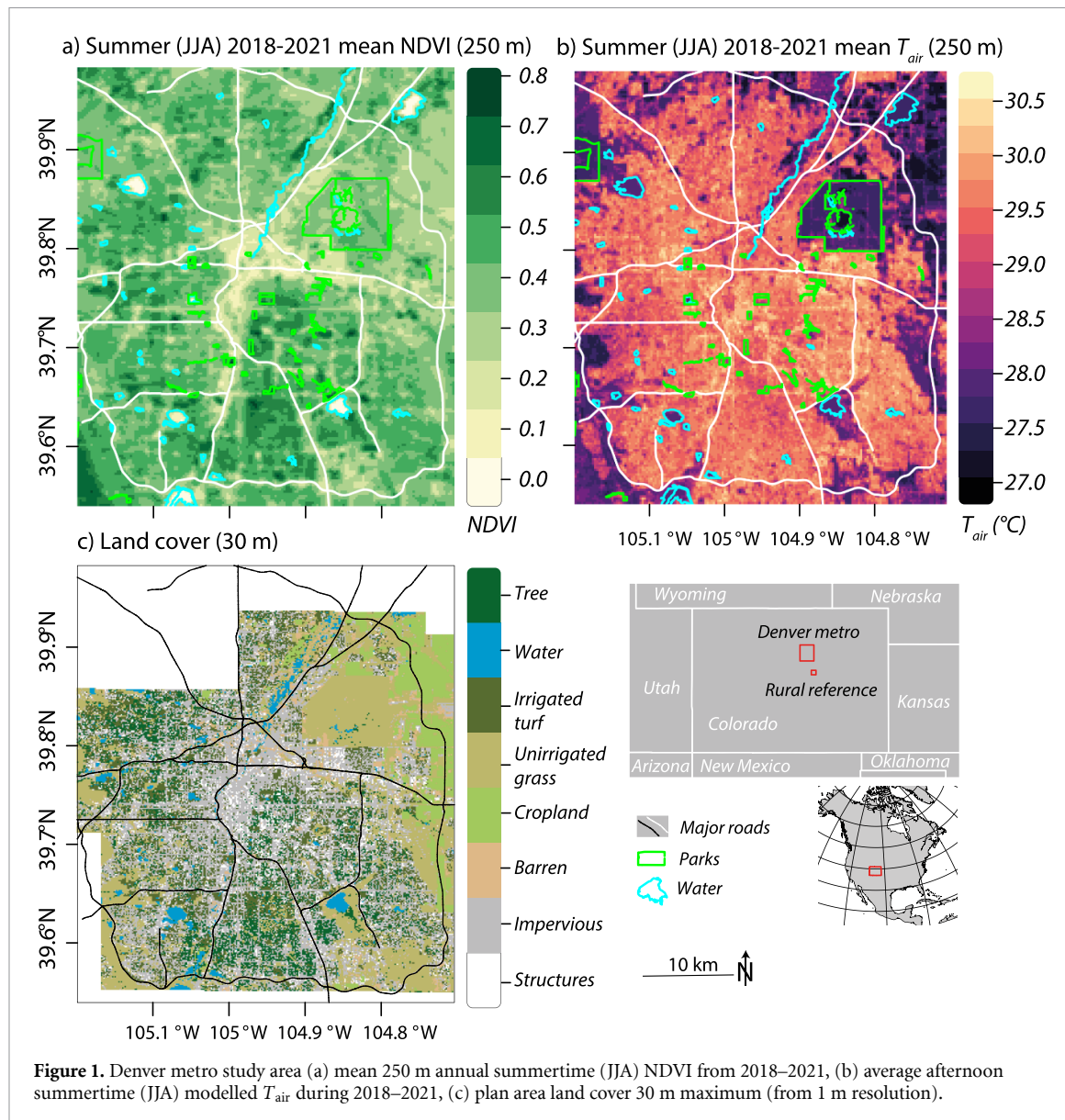
The study period extends from January 2018 to December 2021. Average daily high (low) temperature at Denver International Airport during this period is 19.4 °C (3.2 °C) with average annual rainfall (snowfall) of 286 mm (1300 mm) per year (figure S1). In 2018, the region was characterized by abnormally dry to moderate drought conditions, and during winters 2020–21 and 2021–22, drought conditions were extreme (US Drought Monitor 2022).

To compare with the metro area, a rural reference site was established approximately 30 km from its southern edge (figure 1). The purpose of this reference site is for comparative analysis of phenological timing between the entire metro area and a non-urban location. This area was selected because of its proximity and similar elevation to the metro area, so that it experiences nearly identical background climate trends and synoptic-scale weather events as the metro area. The rural reference area is ~200 km<sup>2</sup> and is characterized by undeveloped grasslands and agriculture, with scattered tree cover at higher elevations and along waterways.

### 2.2. Remotely sensed normalized difference

#### vegetation Index (NDVI) and phenology metrics

Land surface phenology is determined using satellite measurements of (NDVI; Rouse *et al* 1973, Tucker 1979) obtained from the eMODIS collection 6, 250 m vegetation index product, composited in 7 d intervals (Jenkinson *et al* 2010). NDVI data were obtained



for the study area for January 2018 to December 2021 from the USGS EROS archive (182 total images, figure S2). Dates of known snow accumulation during the study period, determined from meteorological records, are removed from the series. NDVI from individual pixels is the integrated response from the mixture of vegetation types and species present in the pixel. Although higher spatial resolution NDVI products are available at various overpass intervals (e.g. Landsat, 16 d; Sentinel-2, five days), we opted for 7 d composite images (from 1–2 d overpass interval scenes) to reduce data gaps and noise caused by cloud cover or atmospheric interference during individual image acquisitions, while maintaining sufficient temporal resolution to resolve seasonal phenology changes. The suitability of MODIS NDVI products for phenology research is well established and they have been widely used for urban applications (e.g. Krehbiel *et al* 2017, Peng *et al* 2017, Meng *et al* 2020, Zhao *et al* 2022).

Growing season thresholds ( $G_T$ ) are determined for each year and for each 250 m pixel as:

$$G_T = 0.5 * (\text{NDVI}_{\max} - \text{NDVI}_{\min}) + \text{NDVI}_{\min}$$

where  $\text{NDVI}_{\min}$  is determined as the maximum winter (DJF) value for each pixel, to represent non-growing season conditions and avoid snow, and  $\text{NDVI}_{\max}$  is the peak NDVI value for each pixel during each calendar year. The 0.5 value corresponds to the timing of the maximum rate of NDVI change during green-up and senescence (Jeong *et al* 2011) and is based on Wang *et al* (2017) and Parece and Campbell (2018) for high-latitude boreal forest and mid-latitude urban environments. This threshold approach is used because it offers a straightforward and widely applied technique for identifying key phenophases, such as the start and end of the growing season, based on changes in vegetation indices. This method allows us to define clear, reproducible criteria

that signal phenological events, making it particularly suitable for fine-scale, multi-temporal datasets. By using this method, we can capture consistent phenological transitions across different land cover types and ensure comparability between urban and natural areas. Additionally, the threshold method is sensitive to vegetation seasonal dynamics in semi-arid urban environments, where phenological changes may be more spatially heterogeneous compared to more humid and non-urban regions. This makes it an appropriate tool for studying the complex interaction between urbanization and landscape phenology in our study area.

For each pixel, the start of the growing season (start of season; SOS) is defined as the first point in time, before the seasonal maximum, when three consecutive NDVI values are greater than  $G_T$ . End of the growing season (end of season; EOS) is the first point in time, after the seasonal NDVI maximum, that three consecutive NDVI values for a given pixel were less than  $G_T$ . The growing season length (length of season; LOS) is computed as EOS-SOS and peak of season (POS) is defined as the date when  $\text{NDVI} = \text{NDVI}_{\max}$ .

To evaluate the uncertainty of satellite-derived NDVI measurements in urban areas with spatially heterogeneous and/or low vegetation land cover fraction, we compare 7 d composite growing season satellite NDVI data with *in situ* observations from a drone-based multispectral camera and point-scale fractional green cover (FGC) observations at two contrasting urban locations (high- and low-vegetation coverage) (SI) (Pantrignani and Ochsner 2015). From April to November, satellite and *in situ* data are correlated (low-vegetation:  $R_2 = 0.76$  satellite vs drone,  $R_2 = 0.57$  satellite vs FGC,  $n = 23$ ; high-vegetation  $R_2 = 0.76$  satellite vs FGC,  $n = 21$ ) indicating satellite-derived measurements are able to detect NDVI changes in a range of urban environments with sparse and variable vegetation cover.

### 2.3. Land cover

Detailed land cover data derived from orthoimages for the metro area are available at 1 m resolution (DRCOG 2019; table 1; figure 1(c)). Structures, defined as human constructions greater than 2 m in height, cover 12% of the area; tree canopy covers 12% of the area and includes deciduous and evergreen vegetation over 5 m in height; irrigated turf (18%) includes actively managed areas such as lawns, parks, cemeteries, golf courses, and sports fields; and prairie/grasslands (26%) are largely unmanaged regions containing native and introduced perennial grasses, herbaceous vegetation, and shrubs. Additional land cover categories are impervious surfaces (27%) and water (7%).

For each 250 m NDVI pixel, individual 1 m land cover surfaces are aggregated into four categories: ‘unirrigated’ (prairie/grassland), ‘built’ (structures

**Table 1.** Plan area land cover fractions in the Denver metro region at 1 m resolution.

Land cover	Plan area coverage (%)
Impervious	27
Unirrigated/natural grassland	26
Irrigated turf	18
Buildings (>5 m)	12
Tree (>2 m)	12
Water	7

**Table 2.** Common tree species in Denver from the Denver tree inventory dataset. Total tree plan area land cover in the study area is 12%.

Genus	Count ( <i>n</i> )	Proportion (%)
Acer	41 198	14.6
Fraxinus	34 851	12.3
Quercus	24 653	8.7
Gleditsia	24 082	8.5
Ulmus	19 399	6.9
Tilia	18 673	6.6
Pinus	17 538	6.2
	<b>180 394</b>	<b>63.7%</b>

and impervious surfaces), ‘irrigated’ (irrigated turf) and ‘tree’. Every 250 m pixel is characterized by the plan area occupied by each of the four land cover categories.

Combined, irrigated and unirrigated grasses comprise nearly half of all land cover in the study area (44%). Common native and introduced short-grass prairie species in the metro area include blue grama (*Bouteloua gracilis*), needle-and-thread grass (*Hesperostipa comata*), crested wheatgrass (*Agropyron cristatum*), and sand dropseed (*Sporobolus cryptandrus*) (Germaine et al 2013). Kentucky bluegrass (*Poa pretensis*) is the most common species in irrigated lawn areas. Grass phenology is expected to vary according to species type, as well as micro-climate controls.

Phenology also varies among tree species and genus. Tree distribution in the study area is characterized using the Denver Tree Inventory, (Colorado Information Marketplace 2023), a vector point dataset of all trees managed by the Department of Parks and Recreation in the City and County of Denver, Colorado. In this dataset there are 283 185 individual trees, with nearly  $\frac{1}{3}$  of all trees belonging to just seven genera (table 2). Based on Moran’s I autocorrelation tests (SI), these genera are distributed in statistically similar proportions across the study area (though overall tree land cover is not distributed evenly) indicating that where trees are present, the mix of tree species is homogenous.

### 2.4. Air temperature

Air temperatures, representative of seasonal mean, afternoon, clear-sky conditions, are modeled for the study area using a predictive random forest machine

learning model. The model inputs are land surface temperature (LST), high resolution land cover (section 2.3), and regional climate parameters, following Ibsen *et al* (2022).

LST data for the air temperature model are from the Thermal Infrared Sensor aboard the Landsat 8 satellite operated by the U.S. Geological Survey (Loveland and Irons 2016). Images are acquired every ~16 d and have a spatial resolution of 30 m. During processing, images are masked for cloud coverage, corrected for atmospheric water content, and overall LST accuracy is 1.52 °C (rmse; Parastatidis *et al* 2017). For this study, 124 total images were acquired, and individual images were averaged to obtain mean seasonal LST (DJF, MAM, JJA, SON) for input to the air temperature model.

Modeled air temperature data was validated against a distributed network of 149 outdoor thermometers (Purple Air, Inc 2023) distributed across the Denver metropolitan area from the year 2021. The Purple Air stations measure air temperature with a shielded, aspirated thermometer (Bosch BME280 and BME680, accuracy ±0.5 °C from 0 °C–65 °C). We assessed the model fit through the adjusted  $R^2$  of a linear regression of the predicted air temperatures against the observed mean sensor measurements for each season ( $R^2$ : DJF = 0.93, MAM = 0.97, JJA = 0.87, SON = 0.96) (see SI for full technical details of the  $T_{\text{air}}$  model).

## 2.5. Soil moisture measurements

To sample soil conditions in the study area, we continuously measured (2 s samples, 10 min averages) soil moisture and temperature (HOBO S-SMC-M005, Onset, Inc., MA, USA) at 10 cm depth in two locations within irrigated and unirrigated cover types: a representative, irrigated residential yard (automatic irrigation every other day from mid-June to mid-October) and an unirrigated, unmanaged natural grassland (Rocky Mountain Arsenal Wildlife Refuge). The irrigated lawn soil sensor was installed from 1 September 2020 through 25 July, 2021 and the unirrigated sensor was installed from 12 May 2021 through to the end of the study.

## 3. Results

### 3.1. Urban vs rural differences

Annual mean NDVI values are comparable between the urban area (0.30) and the rural reference site (0.28) (figure S1). Although urban–rural mean NDVI is comparable, the urban NDVI spatial variability is significantly greater ( $p < 0.01$ ), on average (urban mean spatial standard deviation is 0.10, rural is 0.06).

Growing season timing also varies between the urban and rural sites. On average, the Denver metro growing season length is 12 d longer than the rural reference, a significant difference ( $p < 0.01$ ) driven by

an earlier urban SOS onset of 2 d and a delayed EOS of 10 d (both significant at  $p < 0.01$ ). POS dates are identical between the two locations.

### 3.2. Intra-urban differences

Summertime NDVI values vary spatially across the urban landscape (figure 1(a)). The highest NDVI values (up to 0.8) are found in suburban residential neighborhoods and vegetated city parks during the summer where vegetation land cover fraction (i.e. the proportion of a MODIS pixel occupied by a tree, unirrigated grass, or irrigated turf) is greatest (50%–60%). In contrast, the city center (24%–30% vegetation cover) had the lowest NDVI values during summer (up to 0.4).

Throughout the year, irrigated areas (>3/4 coverage) have the highest annual average NDVI (0.49), followed by tree (0.40), unirrigated (0.27), and built areas (0.18) (figure 2(a)). To compare phenology among land cover categories, NDVI is also expressed as the proportion of maximum NDVI for each category (figure 2(b)). The majority of tree and built areas follow similar seasonal patterns (figures 2(b) and (c)). For both, SOS occurs between mid-May and early June (day 142 ± 8 and 151 ± 15 respectively), POS occurs in early August, and EOS occurs in October to mid-November (day 281 ± 11 and 267 ± 22 respectively). In contrast, SOS in the majority of unirrigated areas occurs slightly earlier (day 137 ± 10), but POS is much earlier in late May, and EOS occurs in mid-September (day 231 ± 25).

As a result, unirrigated areas have a mean LOS of 94 (±25) days, over two months shorter than irrigated areas (166 d ± 30), and several weeks shorter than built areas (117 ± 29 d). The difference in LOS is driven primarily by differences in EOS timing. This contrast equates to appreciable neighborhood-scale differences in mean SOS, POS, EOS, and LOS across the metro area (figure 3). Overall, the SOS is more spatially uniform (s.d. = 19 d) than EOS (s.d. = 40 d).

### 3.3. Physical drivers of phenology variations

Metro area land surface phenology is associated with spatial patterns of  $T_{\text{air}}$  (figure 4(a)). In the majority of unirrigated grass areas, SOS advances 2 d per K warming during spring (MAM). As  $T_{\text{air}}$  increases above 7 °C, mean SOS for all areas begins to retreat. This appears counterintuitive, however, the warmer and more urbanized areas also have a higher proportion of trees (mean 18% tree coverage in areas > 7 °C; 5% in areas < 7 °C), which have a later SOS than unirrigated grass species found in cooler, less built-up areas.

The greatest effect of  $T_{\text{air}}$  is observed with respect to EOS timing (figure 4(c)). Warmer conditions are associated with a later EOS for  $T_{\text{air}}$  below ~17.5 °C (36 d per K), above which  $T_{\text{air}}$  does not influence

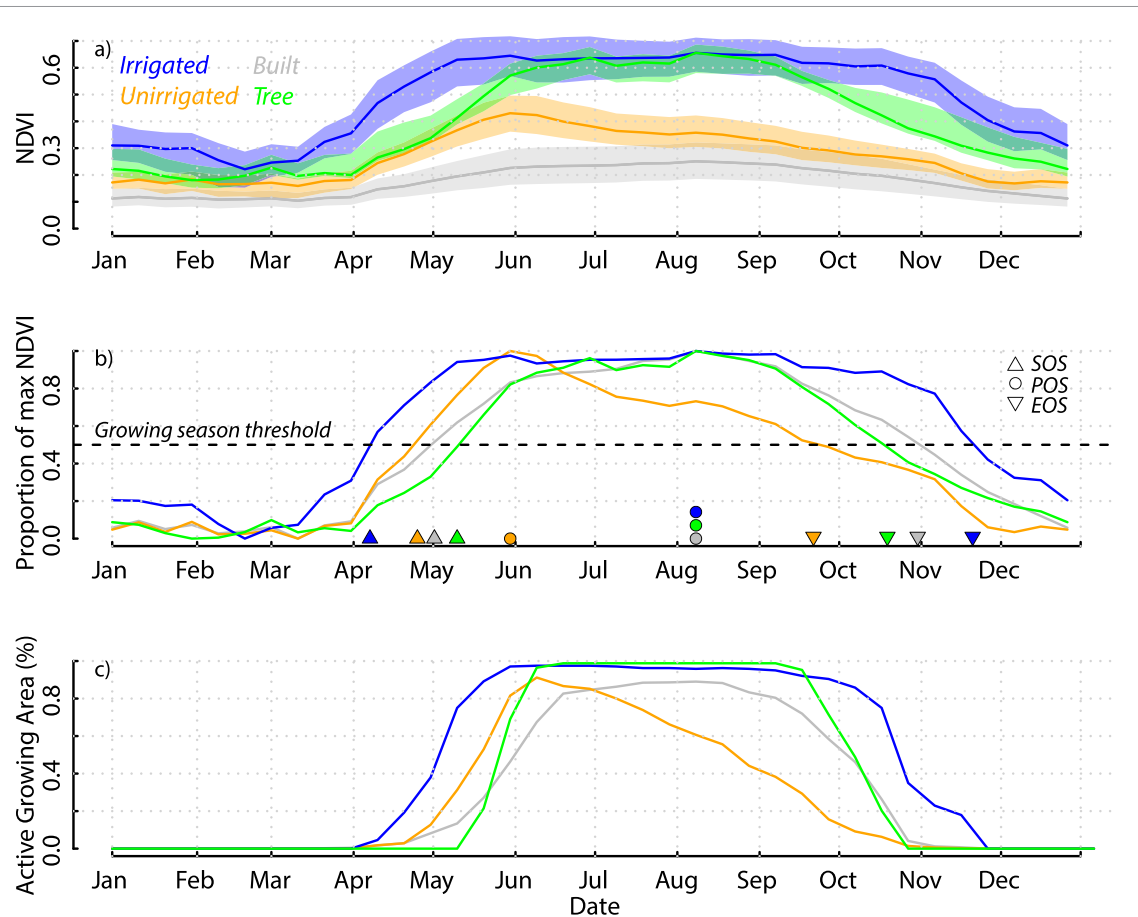


**Figure 2.** (a) Annual NDVI by land cover type using MODIS pixels with  $>2/3$  of pixel area categorized as irrigated, unirrigated or built land cover, or  $>1/2$  of pixel area categorized as ‘tree’ land cover (there are relatively few tree pixels, so the threshold was lowered to have sufficient area for analysis). In the ‘built’ categorization, there is still a fraction of vegetation consisting of tree (5.9%, on average), irrigated turf (8.5%), and unirrigated grass (9.5%). Lines are mean values (2018–2021) in 7 d intervals and shaded areas are the interquartile range. (b) Proportion of maximum NDVI for each land cover type, and the  $0.5 \times$  maximum NDVI threshold that defines SOS and EOS for each land cover type. (c) Percentage area above the growing threshold for each land cover type (all pixels with  $>2/3$  irrigated, unirrigated, built or  $>50\%$  tree cover).

EOS. As with SOS, this trend likely reflects both vegetation physiological response (e.g. majority unirrigated grass areas have extended EOS dates as  $T_{air}$  increases) and a more heterogeneous vegetation mix in warmer, more urbanized areas. Overall, the net impact is that warmer conditions are associated with longer LOS, with a decreasing effect at higher temperature ( $>14.5^{\circ}\text{C}$ ) (figure 4(d)).

The fraction of irrigated and unirrigated land cover (the proportion of a MODIS pixel occupied by each land cover type) is also associated with growing season timing (figures 5(a) and (b)). As the fraction of unirrigated land cover increases, LOS becomes steadily shorter ( $-5$  d per 10% area increase), independent of  $T_{air}$ . This is primarily driven by earlier EOS. In contrast, as irrigated land cover increases, LOS increases (7.7 d per 10% area increase) from both earlier SOS and later EOS dates.

As the built land cover proportion increases (figure 5(d)), SOS is later (2.7 d per 10% increase in built area). Where the built land cover is at a minimum (0%–20%), LOS is reduced (<120 d). In mixed

land cover pixels (built 20%–60%), LOS ( $\sim 140$  d) and EOS dates are relatively constant ( $\sim$ day 280). As the built land cover begins to dominate (built >80%), LOS is truncated at both the beginning and end of the season.

The influence of soil moisture on phenology is also indicated by the correlation between measured monthly mean soil moisture and satellite-observed NDVI at irrigated and unirrigated locations ( $r^2 = 0.47$ ) (figure 6). The unirrigated area has lower soil moisture (7%–22%) and NDVI values (0.2–0.42), while the irrigated area is associated with higher soil moisture (23%–36%) and higher NDVI (0.4–0.56).

To characterize the role of temperature and soil moisture on phenology, growing season dates are compared to  $T_{air}$  and unirrigated land cover (figure 7). In our study region, unirrigated land cover has lower soil moisture than irrigated land cover (figure 6), suggesting that pixels with a greater proportion of unirrigated land cover have lower soil moisture. As with earlier analyses, the largest variation across the study area is found in EOS

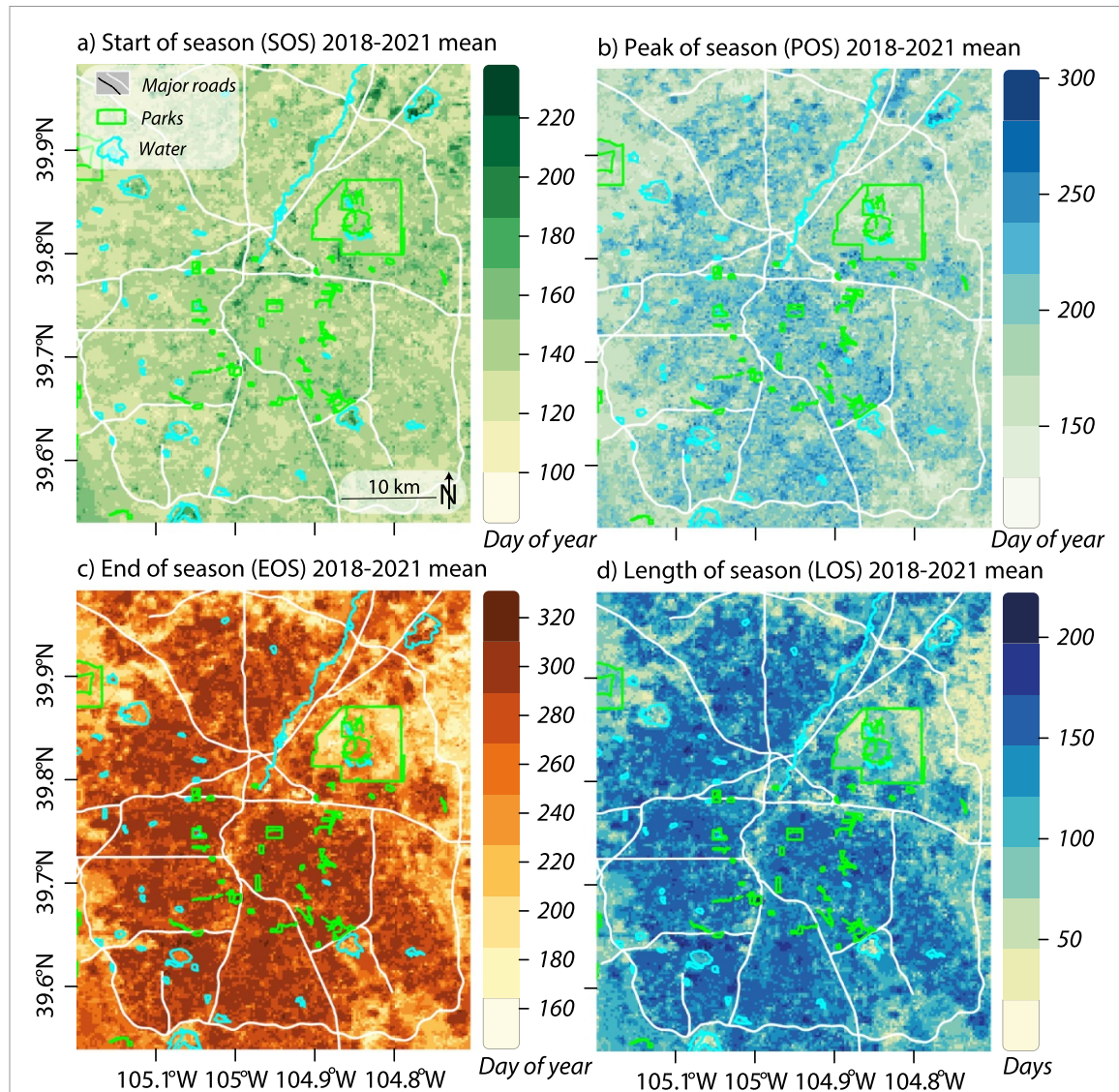


**Figure 3.** (a) start of season (SOS), (b) date of peak NDVI (POS), (c) end of season (EOS), and (d) length of season (LOS). Major parks (green) and bodies of water (blue) are outlined. Images are the mean of 2018–2021 at 250 m grid resolution.

timing (figure 7(c)). Overall, the warmer, wetter areas ( $T_{\text{air}} > 14^{\circ}\text{C}$ , unirrigated land cover  $<0.3$ ) have later EOS dates (day 280–290) and the longest growing seasons (120–150 d). In the cooler, drier areas ( $T_{\text{air}} < 13^{\circ}\text{C}$ ), EOS comes earlier and LOS is shorter.

#### 4. Discussion and conclusions

##### 4.1. Urban vs rural

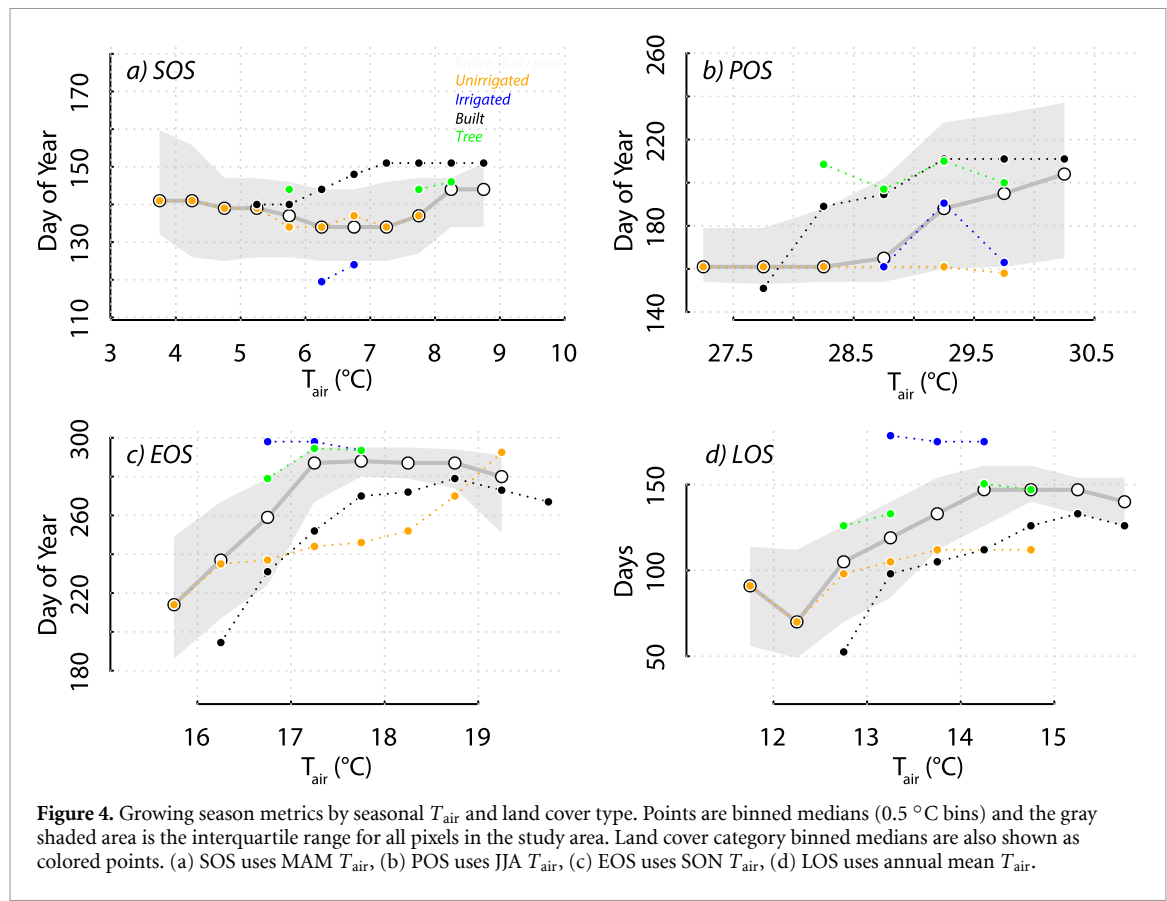
Annual mean NDVI is comparable for the Denver metro area and the rural control (figure S1). This is in contrast to previous studies where urbanization decreases NDVI despite enhanced vegetation growth rates (e.g. Zhao *et al* 2016). However, we did observe higher spatial variation in urban annual NDVI, likely due to the heterogenous patchwork of different vegetation types, densities, and treatments (e.g. irrigation, fertilization) found across the metro landscape.

We also found differences in land surface phenology between urban and rural areas. The LOS in metro Denver is about 12 d longer than the rural control,

consistent with differences of ~8–15 d observed by remotely sensed metrics in other urban–rural comparisons (White *et al* 2002, Meng *et al* 2020, Jochner and Menzel 2015 and refs therein). Our results indicate that the greater LOS in metro Denver is primarily due to delayed EOS, while in many urban areas both vegetation and land surface phenology observations indicate growing season increases due to earlier SOS (White *et al* 2002, Jochner and Menzel 2015, Meng *et al* 2020). The well-documented lengthening of the growing season in urban relative to rural areas is largely attributed to urban heat island effects, but there are other differences, such as greater abundance of exotic species (Shustack *et al* 2009), higher nutrient loading (Jochner *et al* 2013), and changes in hydrology in urban areas (Han and Xu 2013) that may contribute to these differences.

##### 4.2. Intra-urban variability in phenology

Our results identify substantial intra-urban differences in NDVI and in land surface phenology driven



by spatial variability in temperature and land cover type. Within metro Denver, SOS dates are less spatially variable than POS and EOS dates, and as a result, EOS dates are more important drivers of the length of the growing season.

Higher  $T_{\text{air}}$  advances phenology, especially for unirrigated grass, and increases LOS (figure 2). However, our results suggest that the timing of the SOS is only weakly related to  $T_{\text{air}}$ . This result may be due to the highly synchronous timing of the SOS throughout the entire metro area, such that the temporal resolution of the modeled  $T_{\text{air}}$  data ( $\sim 16$  d) is not sufficient to capture variation in green-up dates. This analysis would be improved with matching higher temporal resolution NDVI and LST data. Additionally, frost damage to buds during freeze events in April or May, which occurs most years, may affect the timing of NDVI-derived SOS (Chamberlain and Wolkovich 2021).

$T_{\text{air}}$  has a greater influence on EOS, and thus LOS, than on SOS. Later EOS, POS, and longest LOS occur at intermediate  $T_{\text{air}}$  (figure 4). This result is consistent with the results of Han and Xu (2013) who observed the longest LOS at intermediate LST in urban areas throughout China.

Our results also indicate that intra-urban variation in land surface phenology is associated with irrigation status and land cover type. As landscapes are increasingly dominated by unirrigated land cover, POS and EOS occur earlier and shorten the LOS

(figure 4). Conversely, in landscapes with greater irrigated land cover, LOS increases, driven by both earlier SOS and later EOS. Irrigated urban landscapes typically have higher soil moisture than unirrigated landscapes (Luketich *et al* 2019), suggesting that the urban growing season may be extended by irrigation. Although our study does not include sufficient direct soil moisture measurements in a controlled setting to isolate the role of soil moisture in driving intra-urban variability in phenology, our soil moisture measurements do demonstrate that local NDVI is highly responsive to soil moisture (figure 5), and the relationship is consistent among irrigated and unirrigated cover types. Another potential component of the phenological difference among irrigated and unirrigated areas is related to species differences. Exotic grass species typically have longer growing seasons, and later senescence dates than native species (Wilsey *et al* 2018). Where unirrigated regions are dominated by native species, and irrigated regions by exotics, species differences may also contribute to observed differences in phenology.

Several studies have identified a relationship between impervious surfaces or population density and the length of the growing season due to the effect of urbanization on temperature (Zipper *et al* 2016, Li *et al* 2019). In the current study, urban land surface phenology also varies in response to the amount of built land cover; LOS is greatest in landscapes with intermediate levels of built land cover (30%–70%)

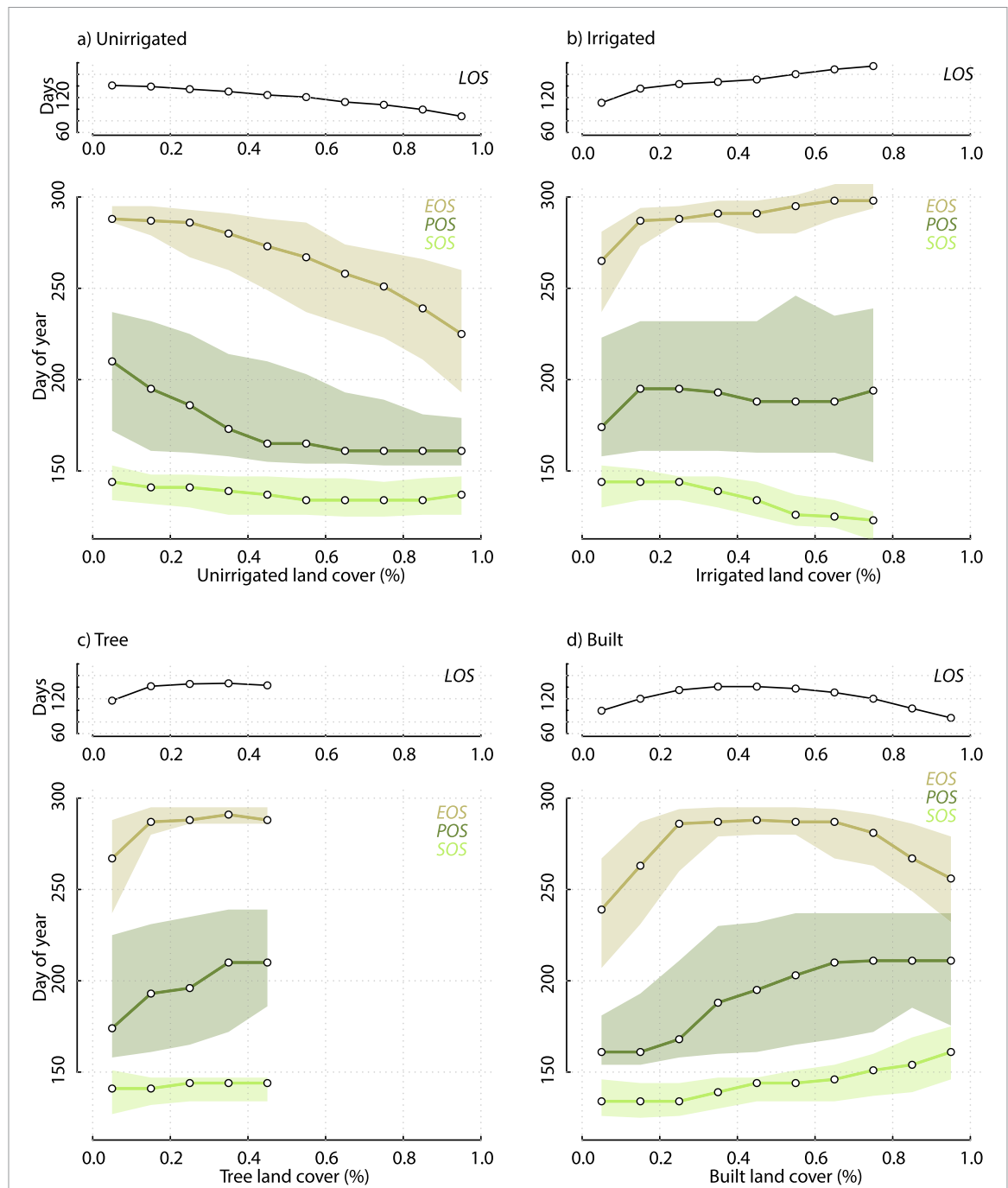
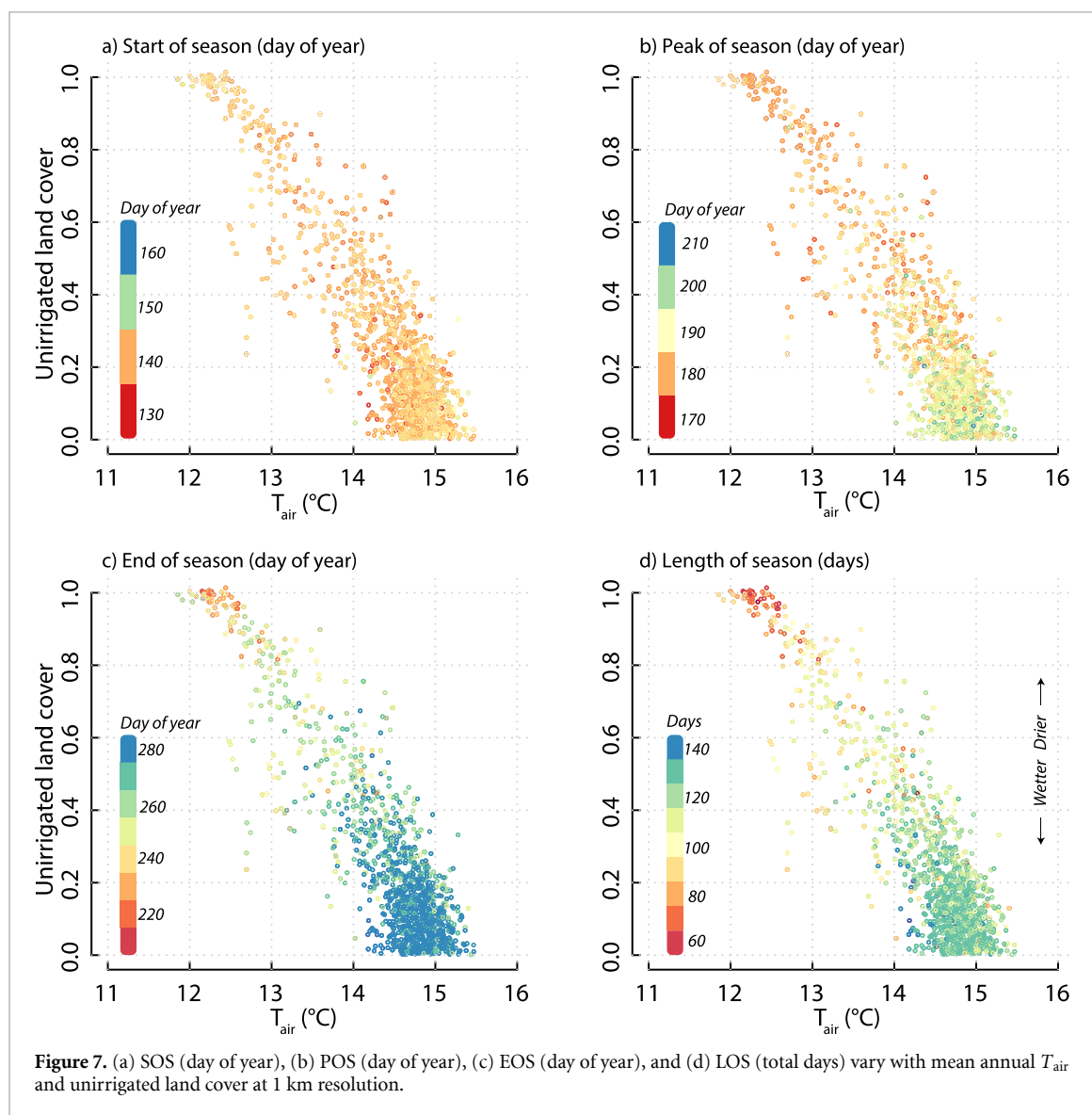
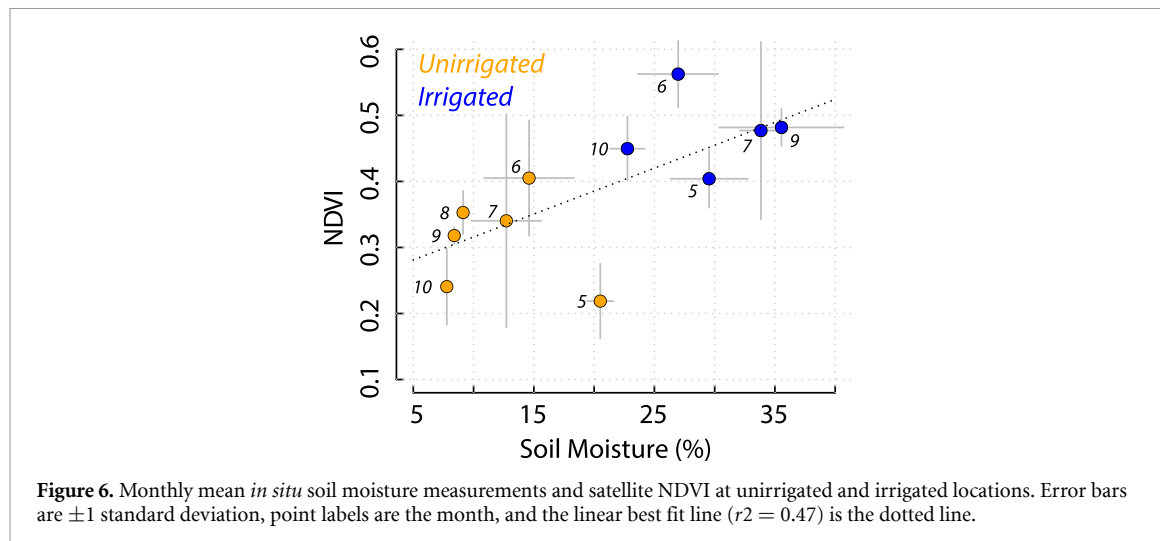


**Figure 5.** Growing season metrics by the proportion of each MODIS pixel occupied by (a) unirrigated land cover, (b) irrigated land cover, (c) trees, and (d) built land cover. LOS is shown in top panels, EOS, POS, and SOS are shown in bottom panels. Points are binned medians (0.1 land cover percentile bins), shaded areas are interquartile range for all pixels.

regardless of  $T_{air}$ . SOS and POS are later where built land cover is greater, however, EOS is latest with intermediate amounts of built land cover. The truncated growing season in areas dominated by built land cover may be due to reduced solar access due to shading from tall buildings (Tan and Ismail 2014), altered hydrology due to impervious surfaces or the impact of environmental pollutants (Manosalidis *et al* 2020). Where there is less built land cover ( $<\sim 30\%$ ), vegetation tends to be unmanaged, so shorter growing seasons are likely due to the prevalence of unirrigated vegetation in these areas as well.

#### 4.3. Climate-vegetation dynamics in water-limited cities

Our results suggest that a unique configuration of environmental drivers are influencing land surface phenology in semi-arid urban environments and that, in addition to air temperature, water availability is an important constraint. Specifically, we observe that higher  $T_{air}$  is not universally associated with a longer growing season, rather that vegetation land cover type and irrigation status are also important controls. Similar results in other non-urban arid and semi-arid environments were explained by a



temperature-induced moisture limitation at the end of the growing season (Liu *et al* 2016, Gonsamo *et al* 2019), but to our knowledge this observation has not been reported for urban environments. Results from Denver are broadly generalizable to other semi-arid

cities, though details will likely vary depending on local vegetation, irrigation infrastructure, water regulations and climate.

Strategic management of vegetation cover can mitigate urban heat at pedestrian to neighborhood

scales by providing shade and enhancing cooling through evapotranspiration, especially in semi-arid regions (Ibsen *et al* 2024). Understanding the relationship between land cover and phenology is a critical component of designing strategies to address urban heat. Our study identifies specific conditions that are conducive for longer growing seasons, and therefore has more potential for cooling of the local environment. We find that irrigated landscapes are associated with longer growing seasons, while unirrigated landscapes are associated with shorter growing seasons in this region (figures 4 and 6). Specifically, warmer, irrigated areas with intermediate levels of built land cover have the longest growing season lengths. Additionally, our results show that different types of vegetative land cover (i.e. irrigated and non-irrigated trees and grasses) exhibit distinct phenological patterns (e.g. Figures 2 and 5) with implications for thermal comfort via shading, evapotranspiration rates, and sensible heat flux. Finally, our findings also highlight the need for distributed soil moisture measurements in cities to characterize soil growing conditions and surface-atmosphere interactions and suggest that irrigation and water management strategies are particularly important tools for managers in semi-arid cities to maximize ecosystem services and benefits from vegetation.

## Data availability statement

The data that support the findings of this study are openly available at the following URL/DOI: <https://doi.org/10.5281/zenodo.14147136>.

## ORCID iDs

- Ben Crawford  <https://orcid.org/0000-0003-3820-7982>  
Kathy Kelsey  <https://orcid.org/0000-0002-4631-8538>  
Peter Ibsen  <https://orcid.org/0000-0002-3436-9100>

## References

- Anderegg W R, Abatzoglou J T, Anderegg L D, Bielory L, Kinney P L and Ziska L 2021 Anthropogenic climate change is worsening North American pollen seasons *Proc. Natl Acad. Sci.* **118** e2013284118
- Beard K H, Kelsey K C, Leffler A J and Welker J M 2019 The missing angle: ecosystem consequences of phenological mismatch *Trends Ecol. Evol.* **34** 885–8
- Chamberlain C J and Wolkovich E M 2021 Late spring freezes coupled with warming winters alter temperate tree phenology and growth *New Phytol.* **231** 987–95
- Cherlet M, Hutchinson C, Reynolds J, Hill J, Sommer S and von Maltitz G (ed) 2018 *World Atlas of Desertification* (Publication Office of the European Union)
- Chmielewski F M and Rötzer T 2001 Response of tree phenology to climate change across Europe *Agric. For. Meteorol.* **108** 101–12
- Denver Regional Council of Governments 2019 *DRCOG high resolution land use/land cover pilot project Working Paper* (Denver Regional Council of Governments) (available at: [https://gis.drcog.org/rdc/supplemental/lulc\\_pilot\\_report.zip](https://gis.drcog.org/rdc/supplemental/lulc_pilot_report.zip)) (Accessed 8 March 2021)
- Denver Tree Inventory, Colorado Information Marketplace 2023 *Tree Inventory Denver* (available at: [https://data.colorado.gov/Natural-Resources/Tree-Inventory-Denver/wz8h-dap6/about\\_data](https://data.colorado.gov/Natural-Resources/Tree-Inventory-Denver/wz8h-dap6/about_data)) (Accessed September 2023)
- Germaine S, Zeigenfuss L C and Schoenecker K A 2013 Bison grazing ecology at the Rocky Mountain Arsenal National Wildlife Refuge *Geological Survey Open-File Report 2013-1112* p 20 (available at: <http://pubs.usgs.gov/of/2013/1112/>)
- Gonsamo A, Ter-Mikaelian M T, Chen J M and Chen J 2019 Does earlier and increased spring plant growth lead to reduced summer soil moisture and plant growth on landscapes typical of Tundra-Taiga interface? *Remote Sens.* **11** 1989
- Han G and Xu J 2013 Land surface phenology and land surface temperature changes along an urban-rural gradient in yangtze River Delta, China *Environ. Manage.* **52** 234–49
- Ibsen P C, Crawford B R, Corro L, Bagstad K J, McNellis B E, Jenerette G D and Diffendorfer J E 2024 Urban tree cover provides consistent mitigation of extreme heat in arid but not humid cities *Sustain. Cities Soc.* **17** 105677
- Ibsen P C, Jenerette G D, Dell T, Bagstad K J and Diffendorfer J E 2022 Urban landcover differentially drives day and nighttime air temperature across a semi-arid city *Sci. Total Environ.* **829** 154589
- Jenkerson C B, Maiersperger T and Schmidt G 2010 EMODIS: A User-friendly Data Source *Open-File Report* pp 10–22
- Jeong S J, CH H O, Gim H J and Brown M E 2011 Phenology shifts at start vs. end of growing season in temperate vegetation over the Northern Hemisphere for the period 1982–2008 *Glob. Change Biol.* **17** 2385–99
- Jochner S, Höfler J, Beck I, Göttlein A, Ankerst D P, Traidl-Hoffmann C and Menzel A 2013 Nutrient status: a missing factor in phenological and pollen research? *J. Exp. Bot.* **64** 2081–92
- Jochner S and Menzel A 2015 Urban phenological studies—past, present, future *Environ. Pollut.* **203** 250–61
- Krehbiel C, Zhang X and Henebry G M 2017 Impacts of thermal time on land surface phenology in urban areas *Remote Sens.* **9** 499
- Lai D, Liu W, Gan T, Liu K and Chen Q 2019 A review of mitigating strategies to improve the thermal environment and thermal comfort in urban outdoor spaces *Sci. Total Environ.* **661** 337–53
- Lesica P and Kittelson P M 2010 Precipitation and temperature are associated with advanced flowering phenology in a semi-arid grassland *J. Arid Environ.* **74** 1013–7
- Li D, Stucky B J, Deck J, Baiser B and Guralnick R P 2019 The effect of urbanization on plant phenology depends on regional temperature *Nat. Ecol. Evol.* **3** 1661–7
- Li X, Zhou Y, Asrar G R, Mao J, Li X and Li W 2017 Response of vegetation phenology to urbanization in the conterminous United States *Glob. Change Biol.* **23** 2818–30
- Liu Q, Fu Y H, Zhu Z, Liu Y, Liu Z, Huang M, Janssens I A and Piao S 2016 Delayed autumn phenology in the Northern Hemisphere is related to change in both climate and spring phenology *Glob. Change Biol.* **22** 3702–11
- Loveland T R and Irons J R 2016 Landsat 8: the plans, the reality, and the legacy *Remote Sens. Environ.* **185** 1–6
- Luketich A M, Papuga S A and Crimmins M A 2019 Ecohydrology of urban trees under passive and active irrigation in a semiarid city *PLoS One* **14** e0224804
- Manalisidis I, Stavropoulou E, Stavropoulos A and Bezirtzoglou E 2020 Environmental and health impacts of air pollution: a review *Front. Public Health* **8** 14
- Melaas E K, Wang J A, Miller D L and Friedl M A 2016 Interactions between urban vegetation and surface urban heat islands: a case study in the Boston metropolitan region *Environ. Res. Lett.* **11** 1–11

- Meng L *et al* 2020 Urban warming advances spring phenology but reduces the response of phenology to temperature in the conterminous United States *Proc. Natl Acad. Sci. USA* **117** 4228–33
- Menzel A and Fabian P 1999 Growing season extended in Europe *Nature* **397** 659
- Mimet A, Pelissier V, Quénol H, Aguejad R, Dubreuil V and Rozé F 2009 Urbanisation induces early flowering: evidence from platanus acerifolia and prunus cerasus *Int. J. Biometeorol.* **53** 287–98
- Myneni R B, Keeling C D, Tucker C J, Asrar G and Nemani R R 1997 Increased plant growth in the northern high latitudes from 1981 to 1991 *Nature* **386** 698–702
- Parastatidis D, Mitraka Z, Chrysoulakis N and Abrams M 2017 Online global land surface TEMPERATURE estimation from Landsat *Remote Sens.* **9** 1208
- Parece T E and Campbell J B 2018 Intra-urban microclimate effects on phenology *Urban Sci.* **2** 26
- Parmesan C and Yohe G 2003 A globally coherent fingerprint of climate change *Nature* **421** 37–42
- Patrignani A and Ochsner T E 2015 Canopeo: a powerful new tool for measuring fractional green canopy cover *Agron. J.* **107** 2312–20
- Peng D, Wu C, Li C, Zhang X, Liu Z, Ye H, Luo S, Liu X, Hu Y and Fang B 2017 Spring green-up phenology products derived from MODIS NDVI and EVI: intercomparison, interpretation and validation using national phenology network and AmeriFlux observations *Ecol. Indic.* **77** 323–36
- Penuelas J, Rutishauser T and Filella I 2009 Phenology feedbacks on climate change *Science* **324** 887–8
- Pretzsch H *et al* 2017 Climate change accelerates growth of urban trees in metropolises worldwide *Sci. Rep.* **7** 1–10
- Purple Air, Inc 2023 PurpleAir (available at: [www2.purpleair.com/](http://www2.purpleair.com/)) (Accessed September 2023)
- Rouse J W, Hass R H, Schell J A and Deering D W 1973 Monitoring vegetation systems in the great plains with ERTS *3rd Earth Resource Technology Satellite Symp.* pp 309–17
- Shustack D P, Rodewald A D and Waite T A 2009 Springtime in the city: exotic shrubs promote earlier greenup in urban forests *Biol. Invasions* **11** 1357–71
- Tan P Y and Ismail M R 2014 Building shade affects light environment and urban greenery in high-density residential estates in Singapore *Urban For. Urban Greening* **13** 771–84
- Tucker C J 1979 Red and photographic infrared linear combinations for monitoring vegetation *Remote Sens. Environ.* **8** 127–50
- US Drought Monitor 2022 *U.S. Drought Monitor* (available at: <https://droughtmonitor.unl.edu/CurrentMap.aspx>) (Accessed July 2022)
- Wang S, Zhang L, Huang C and Qiao N 2017 An NDVI-based vegetation phenology is improved to be more consistent with photosynthesis dynamics through applying a light use efficiency model over boreal high-latitude forests *Remote Sens.* **9** 695
- White M A, Nemani R R, Thornton P E and Running S W 2002 Satellite evidence of phenological differences between urbanized and rural areas of the eastern United States deciduous broadleaf forest *Ecosystems* **5** 260–73
- Wilsey B J, Martin L M, Kaul A D and Firn J 2018 Phenology differences between native and novel exotic-dominated grasslands rival the effects of climate change *J. Appl. Ecol.* **55** 863–73
- Wohlfahrt G, Tomelleri E and Hammerle A 2019 The urban imprint on plant phenology *Nat. Ecol. Evol.* **3** 1668–74
- Zhang X, Friedl M A, Schaaf C B, Strahler A H and Schneider A 2004 The footprint of urban climates on vegetation phenology *Geophys. Res. Lett.* **31** 10–13
- Zhao C, Weng Q, Wang Y, Hu Z and Wu C 2022 Use of local climate zones to assess the spatiotemporal variations of urban vegetation phenology in Austin *GISci. Remote Sens.* **59** 393–409
- Zhao S, Liu S and Zhou D 2016 Prevalent vegetation growth enhancement in urban environment *Proc. Natl Acad. Sci.* **113** 6313–8
- Zipper S C, Schatz J, Singh A, Kucharik C J, Townsend P A and Loheide S P 2016 Urban heat island impacts on plant phenology: intra-urban variability and response to land cover *Environ. Res. Lett.* **11** 054023